



## Adsorption characteristics of antibiotics trimethoprim by activated carbon developed from low-cost alligator weed: kinetics, equilibrium and thermodynamic analyses

Ming-sheng Miao<sup>a,†</sup>, Shuai-shuai Ma<sup>a,b,†</sup>, Li Shu<sup>c</sup>, Qiang Kong<sup>a,b,\*</sup>, Yu-zhen Liu<sup>b</sup>

<sup>a</sup>College of Life Science, Shandong Normal University, 88 Wenhua Donglu, Jinan 250014, Shandong, China, Tel. +86 531 86182550; Fax: +86 531 86180107; emails: kongqiang0531@hotmail.com (Q. Kong), mingshengmiao@163.com (M.-s. Miao), 2410191093@qq.com (S.-s. Ma)

<sup>b</sup>Institute of Environment and Ecology, College of Geography and Environment, Shandong Normal University, 88 Wenhua Donglu, Jinan 250014, Shandong, China, email: 75980079@qq.com

<sup>c</sup>School of Engineering, RMIT University, 402 Swanston Street, Melbourne, VIC 3000, Australia, email: li.shu846@gmail.com

Received 29 January 2017; Accepted 18 June 2017

### ABSTRACT

Low-cost activated carbon was prepared from alligator weed by phosphoric acid activation and employed for the removal of trimethoprim (TMP) from aqueous solutions. The activated carbon content in the alligator weed-activated carbon (AWAC) was 55.38%. Scanning electron microscopy showed that AWAC features a rough surface with highly porous structures consisting of micropores and mesopores. The AWAC had a high surface area of 752.6 m<sup>2</sup>/g and an average pore size of 5.80 nm, which were responsible for its favorable adsorption ability. The AWAC adsorbed ~92% of a 60 mg/L TMP solution. The maximum TMP adsorption capacity was about ~125 mg/g at 298 K. The TMP sorption kinetic data fitted well to the pseudo-second-order kinetic equation ( $R^2 = 1$ ). The Freundlich isotherm gave the best correlation ( $R^2 = 0.9950$ ) with the experimental data at 303 K, indicating multimolecular layer adsorption. Thermodynamics studies revealed that the adsorption process is spontaneous and exothermic. Fourier transform infrared spectroscopy revealed the presence of the AWAC surface functional groups, such as C–H, C–O and C–C moieties. The intensity of the spectral peaks of AWAC decreased after adsorption, owing to reaction of the functional groups with TMP.

*Keywords:* Alligator weed; Activated carbon; Adsorption; Trimethoprim

### 1. Introduction

Environmental pollution problems have grown in tandem with developing industrialization worldwide. Much of the contamination ultimately accumulates in aquatic systems, and contaminants have been detected in both drinking

water and wastewater. Antibiotic contamination has been found in a diverse range of environmental compartments around the world, including wastewater, groundwater and river water, hospital wastewater, sludge, soil and manure [1]. A notable contaminant is trimethoprim (TMP), an antibacterial drug derived from diaminopyrimidine that is commonly used in the prophylactic treatment of urinary, intestinal and respiratory infections [2]. TMP is often poorly metabolized when absorbed by humans and animals, and approximately

\* Corresponding author.

† These authors contributed equally to this work.

Presented at the 9th International Conference on Challenges in Environmental Science & Engineering (CESE-2016), 6–10 November 2016, Kaohsiung, Taiwan.

60% of TMP is eventually discharged into the environment in its original form [3]. This release of TMP into the environment may increase the risk of bacterial resistance to the drug. Management of the disposal of TMP contaminated water is important to minimize the adverse impact of the drug to the environment and the human health.

Numerous methods have been employed to remove TMP from effluents, such as electrochemical oxidation, adsorption and microbial degradation. Adsorption of pollutants in water by activated carbon packed fixed-bed columns has proven to be an economical and effective technique [1]. Adsorption techniques are gaining popularity because of their high efficiency, low-energy requirements and simple process operation. Activated carbon is one of the most widely used materials in water treatment because of its exceptional adsorption properties, large surface area and good corrosion resistance [4]. Organophosphorus compounds have been applied as activated agents for producing activated carbon with surface functional groups that increase surface acidic and enhance the sorption capacities. Phosphoric acidity activation has been well demonstrated as an effective method, with low cost and minimal environmental impact [5].

Several kinds of carbon materials can be used as adsorbents for sewage treatment and numerous raw materials have been used to remove TMP from wastewater, such as montmorillonite K10 [6], green alga *Nannochloris* sp. [7] and lotus stalks [4]. Alligator weed (*Alternanthera philoxeroides*) is a plant native to South America that has now spread worldwide because of its extremely vigorous growth and resistance to control measures [8]. This plant invades agricultural areas and blocks drainage and irrigation channels, causing problems on agricultural land. Another concern is that alligator weed causes water pollution from plant decomposition [9]. Alligator weed was one of the first invasive species listed in China. Biological control is considered the best method for managing this weed because mechanical methods exacerbate the rate of spread [10]. In previous studies, activated carbon prepared from alligator weed showed a high potential for removing heavy metals and antibiotics from aqueous solutions [11], owing to alligator weed containing 4.1% lignin and 20.3% cellulose [12]. Alligator weed can produce large amounts of biomass, which can be used as a raw material to prepare high-efficiency activated carbon. The cost of production of alligator weed-activated carbon (AWAC) was CN¥ 2.1/kg [13]. Preparing a sorbent from alligator weed could utilize this pest as a resource and the sorbent could be used to decrease TMP and other antibiotics in aquatic pollution. To the best of our knowledge, there are no studies reporting the use of AWAC as an adsorbent for removing TMP from effluents.

This study aims to use a highly effective method for preparing activated carbon from alligator weed and investigates the suitability of the sorbent for removal of TMP from solutions. The isotherms, kinetics and thermodynamics of TMP adsorption from aqueous solutions are examined. The adsorption performance of AWAC is investigated by assessing the effects of various parameters, including initial TMP solution concentration, contact time, adsorbent dosage, temperature and pH on the adsorption properties of the AWAC.

## 2. Materials and methods

### 2.1. Materials

TMP (CAS# 738-70-5) was supplied by Sangon Biological Engineering (Shanghai, China). The molecular weight of TMP is 290.32 g/mol and it has a chemical formula of  $C_{14}H_{18}N_4O_3$ . A 60 mg/L stock solution of TMP was prepared by dissolving 0.12 g of TMP in 2,000 mL of distilled water. Distilled water was used throughout for solution preparations. The pH values of solutions were adjusted with 0.1 M HCl and/or 0.1 M NaOH.

### 2.2. Preparation of AWAC

The raw alligator weed biomass was collected from Xiaoqing River in Shandong Province, China. The biomass was washed with copious quantities of de-ionized water to remove impurities and release common ions present in river water, and then sun-dried. Alligator weed segments were pretreated in 2 wt% sodium hydroxide solution for 24 h to remove superficial ash and impurities. The segments were rinsed with distilled water until the washings were neutral and the segments dried at 105°C. The dried segments were subjected to a preoxidation process by heating to 200°C for 1 h, which can change the specific surface area of the material and the oxygen content on the surface of the product. The resulting precursor material was immersed in 85 wt% phosphoric acid solution at a ratio of 1:4 (w/w) for 6 h at room temperature [14]. The resulting sample was then carbonized in a muffle furnace (Yong Guangming Company, Beijing) at 600°C for 1 h. The optimal process above is based on the analysis of costs, adsorption performance and optimal phosphoric acid usage. The resulting activated carbon was cooled to room temperature, cleaned with de-ionized water thoroughly until the pH of the filtrate was 7, and then dried at 105°C for 12 h. Finally, the AWAC was ground into a powder before adsorption experiments [15].

### 2.3. Calculation of AWAC content

The AWAC content ratio ( $Y$ , wt%) reflects the quality of activated carbon in AWAC and is defined as follows:

$$Y = m_1/m_2 \times 100 \quad (1)$$

where  $m_1$  is the mass of the activated carbon obtained and  $m_2$  is the mass of the dry, raw alligator weed material.

### 2.4. Properties of AWAC

The surface structural characteristics of the AWAC were observed via scanning electron microscopy (SEM; SUPRA™ 55, Zeiss Company, Germany). The surface area of the activated carbon plays an important role in adsorption efficiency and was calculated from the Brunauer–Emmett–Teller (BET) nitrogen adsorption–desorption isotherms measured at 77 K using an automated surface area analyzer (Quantachrome, USA). The pore-size distribution of the AWAC was ascertained using density functional theory software provided with the instrument using medium regularization [16]. Fourier transform infrared (FTIR) analysis was undertaken to examine the chemical functional groups present on the

AWAC prepared in this study using a FTIR spectrometer (Thermo Scientific, USA).

### 2.5. Sorption studies

The absorption efficiency of the AWAC was examined in batch sorption experiments. TMP solutions of varying concentrations were prepared by dilution of the stock solution with distilled water. The adsorption experiments were performed by agitating 0.05 g AWAC in 50 mL of TMP solution on a temperature-controlled oscillator set at 180 rpm to reach adsorption equilibrium time. Each experimental condition was performed in triplicate, and distilled water used as a blank control. After the adsorption experiment, the solution was passed through a 0.22  $\mu\text{m}$  filter membrane and the absorbance was detected. The concentration after adsorption was determined by referring to the standard curve [14]. The concentrations of TMP in the supernatant solutions before and after sorption were determined using a UV–visible spectrophotometer (T6-Xinshiji, Beijing) at the maximum TMP absorption wavelength of 271 nm.

The TMP uptake at equilibrium  $Q_e$  (mg/g) and the removal rate were calculated using the following equations:

$$Q_e = (C_o - C_e) V/W \quad (2)$$

$$\text{Removal (\%)} = ((C_o - C_e)/C_o) \times 100\% \quad (3)$$

where  $C_o$  is the TMP concentrations prior to the start of the adsorption process,  $C_e$  (mg/L) is the TMP concentrations at equilibrium,  $V$  (L) is the volume of the TMP solution and  $W$  (g) is the mass of the adsorbent.

### 2.6. Batch adsorption experiments

Batch adsorption experiments were performed to study the influence of initial TMP concentration, AWAC dose, solution pH, contact time and temperature of reaction on the adsorption uptake. The pH of the adsorbent was maintained with 0.1 M HCl or 0.1 M NaOH. Kinetics is important for studying adsorption processes and provides a means to understand the adsorption rate and adsorption mechanism. Data obtained from kinetic experiments for the removal of TMP by AWAC were analyzed with pseudo-first-order, pseudo-second-order and intraparticle diffusion models to explain the adsorption mechanism. A 0.05 g dose of AWAC was added to each conical flask containing 50 mL of TMP solution at 30, 60 and 90 mg/L concentrations at initial pH of 3.15. The mixtures were agitated on a temperature-controlled oscillator set at 25°C and 180 rpm. Contact times ranged from 10 to 360 min. The removal rate and adsorption amount of each experiment were calculated and are discussed in the following section.

An adsorption isotherm curve was plotted to express the relationship between temperature and the amount of solute molecules when adsorption had reached equilibrium at two concentrations. Adsorption isotherm studies were performed with eight different initial concentrations of TMP from 20 to 160 mg/L at initial pH of 3.15, contact time 4 h, and an AWAC dosage of 1.0 g/L. The removal rate and adsorption amount were calculated and are discussed in the following section.

## 3. Results and discussion

### 3.1. Characterization of AWAC

#### 3.1.1. SEM characterizations

The surface properties of AWAC before and after adsorption were examined by SEM, and the results are shown in Figs. 1(a) and (b), respectively. Developed apertures exist on the surface of the AWAC, and the apertures are not of uniform size. The number of pores decreased after adsorption of TMP (Fig. 1(b)), with many of the large pores filled with the adsorbate. These large pores and increased surface area are important factors that could cause the high uptake of TMP seen in this study [17]. The carbon activated with phosphoric acid had high adsorption ability under oxidation conditions and phosphoric acid activation may play an important part in the formation of pores. It is generally accepted that the porosity is generated with phosphoric acid remaining intercalated in the internal structure of lignocellulosic materials [18]. As oxidant agents at high temperature, phosphoric acid will release some radicals. These radicals may react with

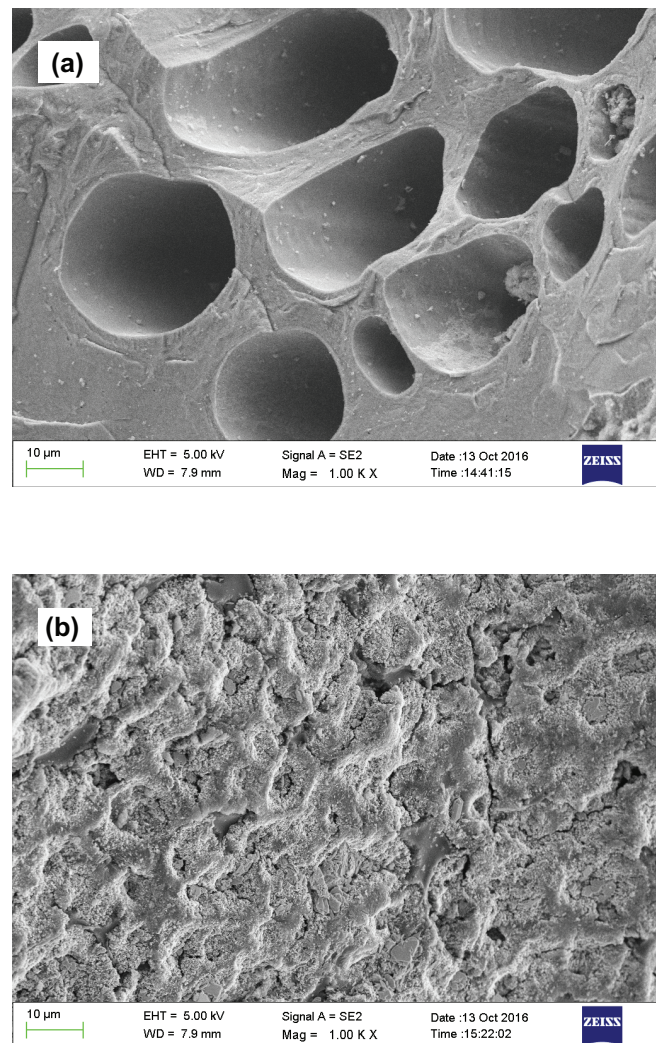


Fig. 1. Scanning electron microscopy images of AWAC (a) before and (b) after TMP adsorption.

precursor and accelerate the formation of new pores and functional groups on precursor [19].

3.1.2. BET and pore-size analysis

The N<sub>2</sub> adsorption isotherm and pore-size distribution of AWAC are shown in Figs. 2(a) and (b), respectively. From Table 1, the S<sub>BET</sub> and V<sub>tot</sub> of AWAC were greater than those of three other activated carbons, concluding that AWAC has better application prospects than the other activated carbons [20–22]. The N<sub>2</sub> volume adsorbed by AWAC continued to increase with increasing P/P<sub>0</sub> after the micropore volume was filled (Fig. 2(a)). The shape of the N<sub>2</sub> adsorption/desorption isotherm was a mixture of types I and IV, with a wider hysteresis loop at high relative pressures, suggesting that AWAC has a mixed microporous and mesoporous structure [23]. The pore-size distribution in the AC indicates that the majority of pores were mesopores (2–10 nm), together with micropores (diameter <2 nm) distributed on the AC surface; no macropores (diameter >50 nm) were present [24]. The ordered mesoporous and microporous structures can promote the

diffusion of ions and improve charge accumulation, therefore, resulting in porous carbon with a high surface area [25]. The AWAC has a developed porous structure that included mainly of micropores and mesopores (Fig. 2(b)). This pore distribution could improve the adsorption capacity of small molecules by AWAC. The BET surface area of the AWAC was determined as 752.6 m<sup>2</sup>/g, and the average pore size was 5.80 nm. These two values reveal that the adsorbent may have favorable adsorption properties [26].

3.2. Adsorption studies

3.2.1. Effect of TMP initial concentration

The effect of initial TMP solution concentration was investigated at five initial concentrations (20, 40, 60, 80 and 100 mg/L) and showed that the adsorption capacity of AWAC increased steadily with increasing TMP solution concentration (Fig. 3). The reason for this is because the effective surface area and the ratio of adsorbate to adsorbent were increased [27]. However, the removal rate of TMP declined with a roughly in a linear trend with increasing TMP initial concen because the number of vacant active sites was limited and the vacant surface sites were difficult to be occupied.

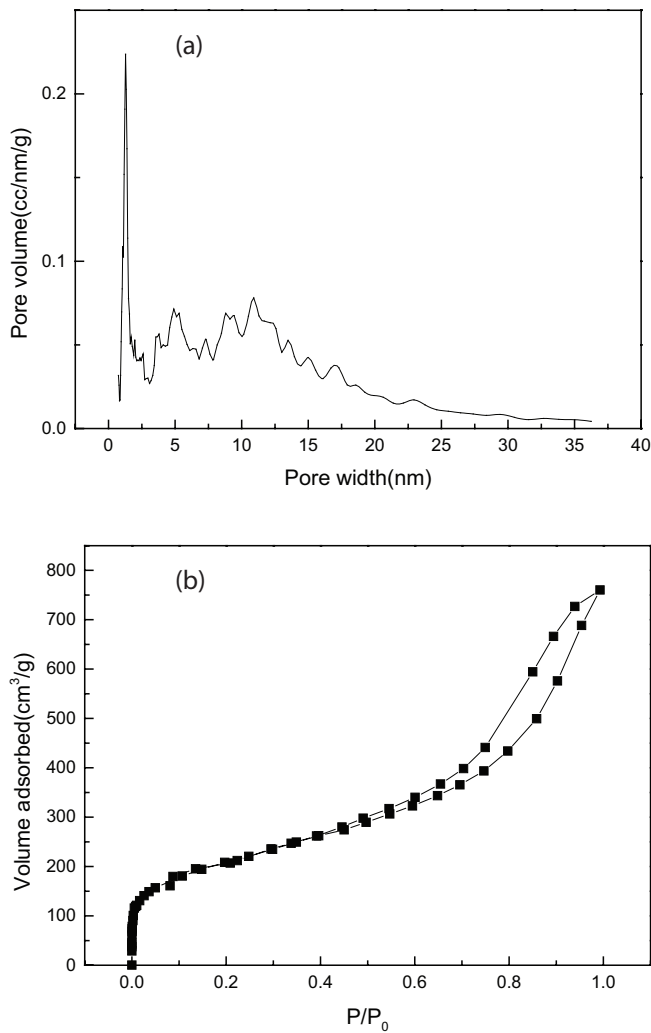


Fig. 2. N<sub>2</sub> adsorption isotherm for AWAC (a) and pore-size distribution curve (b) of alligator weed before adsorption.

Table 1  
Surface area and pore volume parameters of DSAC, AWAC, ALAC and AC-PER

Samples	S <sub>BET</sub> (m <sup>2</sup> /g)	V <sub>tot</sub> (cm <sup>3</sup> /g)	D <sub>p</sub> (nm)	Reference
DSAC	315	0.346	1.35	[20]
AWAC	752	1.09	5.80	This work
AC-PER	342	0.273	3.19	[21]
ALAC	675	0.31	1.85	[22]

DSAC, doum stone-activated carbon; AWAC, alligator weed-activated carbon; ALAC, *Arundo donax* Linn-activated carbon; AC-PER, Lotus stalks-activated carbon; S<sub>BET</sub>, the BET specific surface area; total pore volume (V<sub>tot</sub>), D<sub>p</sub> (average pore diameter) it was calculated as D<sub>p</sub> = 4 V<sub>tot</sub>/S<sub>BET</sub>

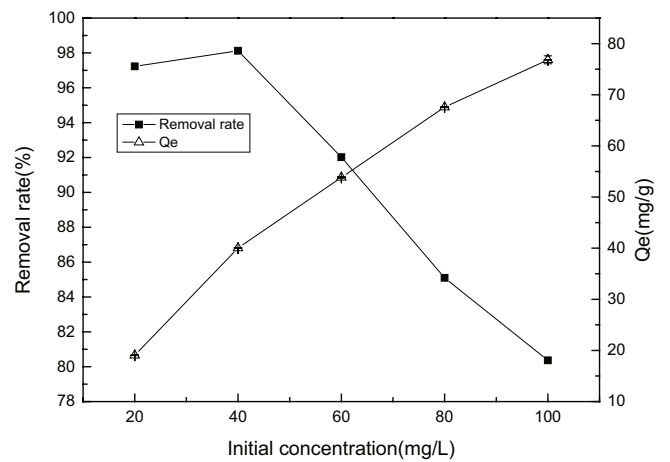


Fig. 3. Effect of initial TMP solution concentration on removal rate and adsorption capacity for five initial concentrations (20, 40, 60, 80 and 100 mg/L, contact time 4 h, AWAC dosage 1.0 g/L, initial pH, shaking speed 180 rpm and temperature 25°C).

### 3.2.2. Effect of contact time

A study of the effect of contact time on the adsorption of TMP by AWAC was performed. Removal rate of TMP at equilibrium decreased from 97% to 73% (Fig. 4). The adsorption process was initially rapid and then increases gradually up to the equilibrium attained at 4 h for all experiments. From this sorption behavior it was concluded that TMP uptake followed a two-step mechanism, where the antibiotics were chemically up taken onto the surface of the AWAC before being taken up into the inner adsorption sites [28]. The first step, known as passive surface transport, took place quite rapidly and adsorption process was fast for the first 30 min. The second passive diffusion transport step took a much longer time for completion [29]. The removal rate of TMP came near to 90% after 4 h. The adsorption process was extended to 6 h to determine the equilibrium contact time. Satisfactory removal had occurred after 4 h, and selecting 4 h in subsequent adsorption experiments as the adsorption equilibrium time.

### 3.2.3. Effect of AWAC dosage

The effect of the adsorbent dose on the adsorption capacity of AWAC and removal efficiency was assessed. AWAC dosages were varying from 0.6 to 2.2 g/L were studied using a TMP solution of 60 mg/L at 298 K (Fig. 5). The removal efficiency increased with increasing AWAC dosages to a point and thereafter remained unchanged. At equilibrium, the removal rate increased from 72% to 99% for an increase in dose from 0.6 to 2.2 g/L. The increase in TMP removal percentages was because of the increase in the available adsorption surfaces and sites. The adsorption capacity of the AWAC decreased as the adsorbent dose increased. After considering the removal rate and adsorption capacity, an AWAC dosage of 1.0 g/L was chosen for subsequent equilibrium experiments.

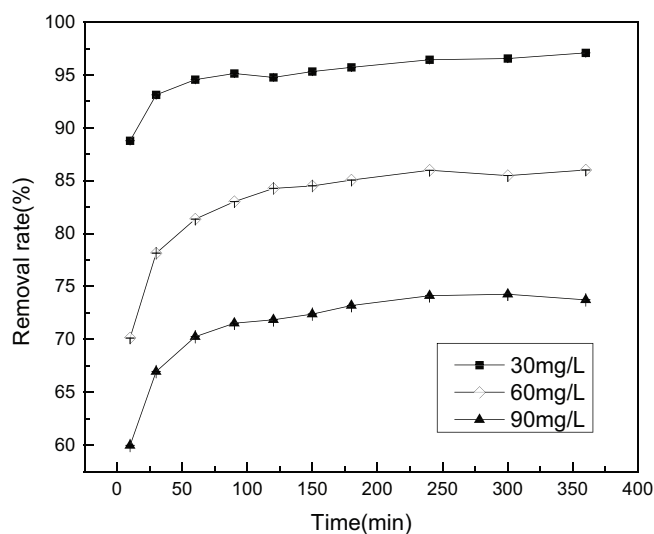


Fig. 4. Effect of contact time on the adsorption of trimethoprim by selected adsorbents (initial trimethoprim concentration are 30, 60 and 90 mg/L, AWAC dosage 1.0 g/L, initial pH, shaking speed 180 rpm and temperature 25°C).

### 3.2.4. Effect of solution pH

The effect of pH on TMP removal was examined by varying the solution pH between 2 and 12. The removal rate of TMP ranged from 59% to 94%, and adsorption capacity of AWAC increased with increasing initial solution pH from acidic to alkaline (Fig. 6). The point of zero charge ( $\text{pH}_{\text{pzc}}$ ) is the most important parameters in the pH study of adsorbents. The  $\text{pH}_{\text{pzc}}$  of AWAC was determined by the following procedure: 50 mL aliquots of a 0.01 N NaCl solution were charged to eight 100-mL conical flasks. The pH values of the solutions were adjusted to values between 2 and 12, and 0.05 g of AWAC added to each flask. The final pH of each solution was measured after 24 h contact time. The difference between initial and final pH ( $\text{pH}_f - \text{pH}_i$ ) was plotted against the initial pH ( $\text{pH}_i$ ) and the point where  $\text{pH}_f - \text{pH}_i = 0$  was taken as the  $\text{pH}_{\text{pzc}}$  [8].

The  $\text{pH}_{\text{pzc}}$  for the AWAC was about 3.9. The structural formula of TMP is shown in Fig. 7. TMP has two amino groups ( $-\text{NH}_2$ ), which may be positively or uncharged.

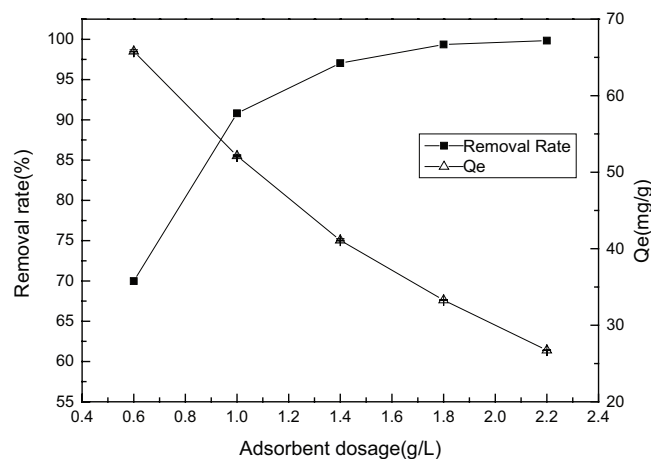


Fig. 5. Effect of AWAC dosage on removal rate and adsorption capacity (TMP concentration 60 mg/L, contact time 4 h, AWAC dosage 1.0 g/L, initial pH, shaking speed 180 rpm and temperature 25°C).

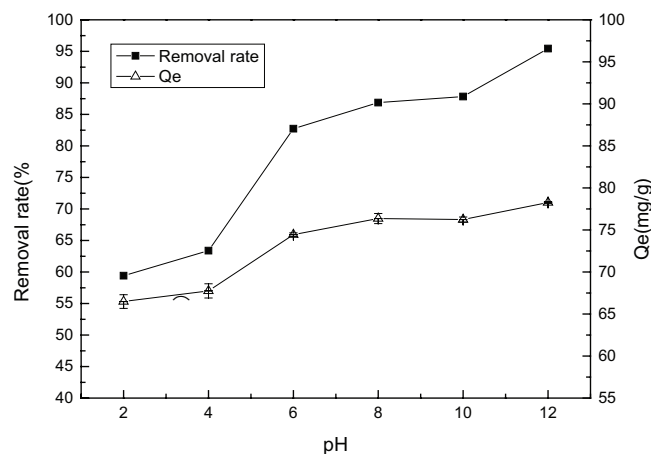


Fig. 6. Effect of solution pH on TMP removal rate and adsorption capacity (TMP concentration 60 mg/L, contact time 4 h, AWAC dosage 1.0 g/L, shaking speed 180 rpm and temperature 25°C).

The surface of the AWAC is positively charged at low pH (2–4,  $\text{pH} < \text{pH}_{\text{pzc}}$ ) and repels the partially protonated TMP ( $\text{TMPH}_2^{2+}$  or  $\text{TMPH}^+$ ), resulting in low sorption. The adsorption process was fast as pH increased above this point ( $\text{pH} > \text{pH}_{\text{pzc}}$ ) because the surface of the activated carbon became negatively charged, which was favorable for the sorption of cationic species ( $\text{TMPH}_2^{2+}$  or  $\text{TMPH}^+$ ) [30]. The pH value had a remarkable influence on TMP adsorption and sorption changed drastically from acidic to alkaline conditions. In order to explore the influence of other factors preferably and reduce the error in the process of experiment, we conducted tests at initial pH in subsequent adsorption experiments.

### 3.2.5. Effect of temperature

Temperature was a key parameter that was studied in the adsorption of TMP to AWAC. The removal rate of TMP by AWAC decreased slightly from 86% to 78% when the temperature increased from 20°C to 40°C, and adsorption capacity gradually decreased (Fig. 8). This shows that the adsorption is an exothermic reaction. The adsorption process involves TMP adsorbing to the surface of AWAC, and free energy of the TMP is decreased. The decrease in adsorption uptake with the rise of temperature may be attributed to weakening adsorptive forces between the active sites of the adsorbent and adsorbate species as well as between the adjacent molecules of the adsorbed phase [31].

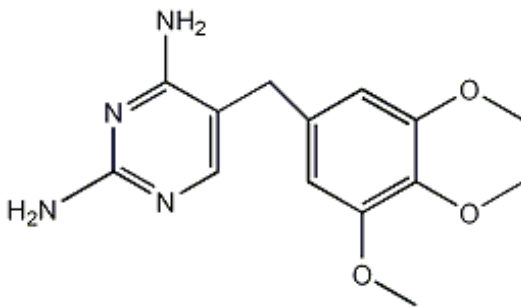


Fig. 7. Molecular structure of trimethoprim (TMP).

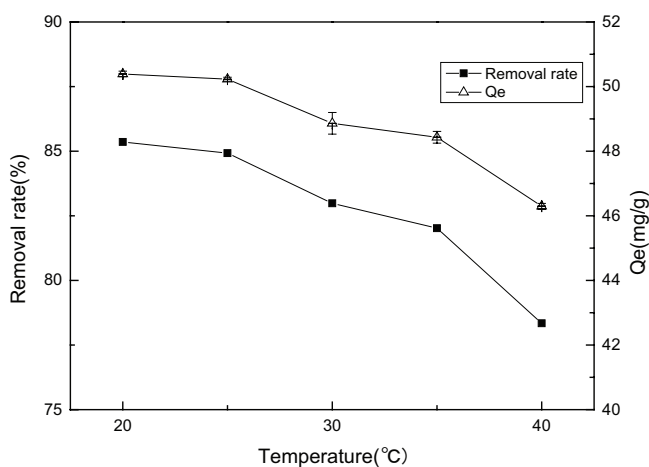


Fig. 8. Effect of temperature on removal rate and adsorption capacity (TMP concentration 60 mg/L, contact time 4 h, AWAC dosage 1.0 g/L, initial pH and shaking speed 180 rpm).

### 3.3. Kinetic models

Pseudo-first-order, pseudo-second-order and intraparticle diffusion models were employed to assess the TMP removal experimental kinetic data.

The pseudo-first-order kinetic model is widely used for the description of adsorption dynamics in aqueous solutions. A linear form of pseudo-first-order model is expressed as follows:

$$\ln(Q_e - Q_t) = \ln Q_e - k_1 t \quad (4)$$

where  $Q_t$  (mg/g) is the sorption capacity at time  $t$  (min) and  $k_1$  (1/min) is the rate constant of the pseudo-first-order model. The values of  $Q_e$  and  $k_1$  can be obtained from the intercept and slope of a plot of  $\ln(Q_e - Q_t)$  vs.  $t$ , respectively.

The pseudo-second-order kinetic model is also widely used for the description of adsorption dynamics in aqueous solutions. This model assumes that the adsorption is a pseudo-chemical reaction process. This model describes the whole process of adsorption and considers the mechanism of adsorption as the limiting factor of adsorption. The pseudo-second-order model is given as follows:

$$t/Q_t = 1/k_2/Q_e^2 + t/Q_e \quad (5)$$

where  $k_2$  (g/(mg min)) is the rate constant and  $V_0$  (mg/(g min)) represents the initial sorption rate. The values of  $Q_e$  and  $k_2$  can be established from the plot of  $t/Q_t$  vs.  $t$ .

Intraparticle diffusion is an important process when passing of an adsorbate from the solution to solid phase is the controlling step of the adsorption. The intraparticle diffusion model can be expressed in linear form as follows:

$$Q_e = k_p t^{0.5} + C \quad (6)$$

where  $k_p$  (mg/(g min<sup>0.5</sup>)) is the intraparticle diffusion rate constant and  $C$  (mg/g) is a constant. Both  $k_p$  and  $C$  can be obtained from the plot of  $Q_e$  vs.  $t^{0.5}$ . Intraparticle diffusion is considered as the sole rate-limiting step if the plot of  $Q_e$  vs.  $t^{0.5}$  is a straight line that passes through the origin.

The corresponding parameters are summarized in Table 2 at initial TMP concentrations of 30, 60 and 90 mg/L using 0.05 g of adsorbent. The experimental data had an excellent fit to pseudo-second-order model, with correlation coefficient ( $R^2$ ) values of 0.999, 1 and 1 when the initial TMP solution concentrations were 30, 60 and 90 mg/L, respectively. The theoretical values of equilibrium sorption capacity ( $Q_{e,\text{cal}}$ ) agreed well with the experimental values ( $Q_{e,\text{exp}}$ ), further suggesting that the sorption of TMP follows the pseudo-second-order kinetic equation and indicating the rate-limiting factor was bond formation between the TMP and AWAC [20].

### 3.4. Adsorption isotherms

Studying the adsorption isotherm is worthwhile to understand the complex mechanism of interaction between the adsorbate and adsorbent. The isotherm reveals the relationship between equilibrium adsorption and solution concentration when equilibrium is reached at certain temperatures. The adsorption isotherm can reflect how the

adsorbate molecule is distributed and transferred between liquid and solid phases in the process of adsorption equilibrium. The isotherm results were analyzed by fitting the equilibrium adsorption data to Langmuir, Freundlich and Dubinin–Radushkevich models.

The Langmuir model is related to the assumption that maximum sorption corresponds to saturation of solute molecules with no lateral interaction between adsorbed molecules. The Langmuir model is mainly used to describe monolayer adsorption processes. The linearized Langmuir equation is applied in the present work as follows:

$$C_e/Q_e = 1/Q_m k_L + C_e/Q_m \quad (7)$$

where  $Q_m$  (mg/g) is the maximum capacity of TMP adsorption and  $k_L$  (L/mg) is the Langmuir constant that is related to the energy of adsorption.

The Freundlich isothermal adsorption model is an empirical formula derived from experimental results. This isothermal model was hypothesized based on a different surface at each point in the adsorption surface, and this model is used widely in the study of adsorption from solution. This model can be expressed as follows:

$$Q_e = k_F C_e^{1/n} \quad (8)$$

where  $k_F$  is the Freundlich constant (mg/g) and  $n$  is the adsorption intensity. Adsorption capacity is represented by  $1/n$  and a small  $1/n$  value indicates high adsorption performance. The values of  $k_F$  and  $1/n$  are calculated using the intercept and slope of the fitted line.

The Dubinin–Radushkevich model is an equation that measures adsorbent micropore volume using the low and medium voltage parts of the adsorption isotherm. It is based on the invariance of the adsorption characteristic curve with temperature. The model is represented by the following equations:

$$\ln Q_e = \ln Q_m - \beta \varepsilon^2 \quad (9)$$

$$\varepsilon = RT \ln(1 + 1/C_e) \quad (10)$$

$$E = 1/(2\beta)^{1/2} \quad (11)$$

where  $\beta$  (kJ<sup>2</sup>/mol<sup>2</sup>) is the constant relating to the adsorption energy,  $\varepsilon$  is the Polanyi potential,  $R$  is the thermodynamic constant and  $E$  (kJ/mol) is the average free energy of adsorption.

The equilibrium isotherm is described by a sorption isotherm, which is characterized by certain constants whose values express the surface properties, and the affinity of the sorbent sorption equilibrium is established when the concentration of sorbate in the bulk solution is in dynamic balance with that at the sorbent interface [32]. The adsorption process was determined by matching experimental data with the three adsorption models. The relevant parameters are shown in Table 3, indicating the maximum adsorption capacity of TMP by AWAC was ~125 mg/g at 298 K. Experimental data showed a favorable fit to both the Langmuir and Freundlich models ( $R^2 = 0.986$  and  $0.995$ ), and a poor fit to the Dubinin–Radushkevich model ( $R^2 = 0.771$ ). The experimental adsorption data fitted best to the Freundlich model, indicating that adsorption of TMP was multimolecular layer adsorption (Fig. 9) [33]. This adsorptive behavior implies that the surface of AWAC is heterogeneous. The heterogeneity may be attributed to the various functional groups on the activated carbon surface and the various adsorbent–adsorbate interactions [23]. Comparing the adsorption capacity of AWAC with other low-cost activated carbon adsorbents in Table 4 [6,34,35], the results showed that alligator weed have favorable potential as an adsorbent material source for TMP removal from effluent.

Table 2

Kinetic parameters of the pseudo-first-order, pseudo-second-order and particle diffusion model for the adsorption of TMP by AWAC

Concentration (mg/L)	Experimental data $Q_e$ (mg/g)	Pseudo-first-order kinetics			Pseudo-second-order kinetics				Particle diffusion model		
		$k_1$ (min <sup>-1</sup> )	$Q_e$ (mg/g)	$R^2$	$k_2$ (g/(mg g))	$Q_e$ (mg/g)	$V_0$ (mg/(g min))	$R^2$	$k_p$ (mg/(g min <sup>0.5</sup> ))	$C$ (mg/g)	$R^2$
30	29	0.011	2	0.8310	0.016	29	14.08	0.999	0.12	26.29	0.7760
60	52	0.015	8	0.9610	0.005	52	14.08	1	0.51	43.03	0.7580
90	66	0.016	11	0.9560	0.004	67	18.87	1	0.67	55.63	0.7370

Table 3

Langmuir, Freundlich, Dubinin–Radushkevich model and correlation coefficients for adsorption of TMP onto AWAC

Temperature (K)	Langmuir model			Freundlich model				Dubinin–Radushkevich model		
	$Q_m$ (mg/g)	$k_L$ (L/mg)	$R^2$	$1/n$	$k_F$ (mg/g) <sup>1/n</sup>	$R^2$	$\beta$ (mol <sup>2</sup> /J <sup>2</sup> )	$Q_m$ (mg/g)	$E$ (kJ/mol)	$R^2$
298	125	0.072	0.905	3.650	28.818	0.946	0.053	68.786	3.071	0.581
303	83	0.180	0.986	4.545	30.205	0.995	0.039	61.252	3.581	0.771
308	83	0.177	0.987	0.206	30.723	0.987	0.030	60.039	4.082	0.710

3.5. Adsorption thermodynamics

Thermodynamics is a science that studies energy conversion in processes. The Gibbs free energy of a process can be judged by whether the process occurs spontaneously in a closed system. If the Gibbs free energy change  $\Delta G$  (kJ/mol) is negative it indicates that the reaction is spontaneous. If the enthalpy  $\Delta H$  (kJ/mol) is positive then the process is an endothermic reaction. It can be expressed as follows:

$$\ln k_L = \Delta S^\circ/R - \Delta H^\circ/RT \tag{12}$$

$$\Delta G^\circ = -RT \ln k_L \tag{13}$$

where  $\Delta G^\circ$  is the standard Gibbs free energy change,  $\Delta H^\circ$  is the enthalpy change and  $\Delta S^\circ$  is the entropy change. These parameters can be related to the level of feasibility and nature of the adsorption process.

Thermodynamic parameters such as free energy change, enthalpy change and entropy were calculated to evaluate the thermodynamic feasibility and the spontaneous nature of the adsorption [36]. The relevant thermodynamic coefficients are shown in Table 5, which show the negative values of Gibbs free energy decreased with increasing the temperature. This indicates the sorption is spontaneous and feasibility of the adsorption via physical forces as well as high tendency of the adsorbent for the adsorbate [37]. The  $\Delta H$  was negative, indicating the adsorption process is

exothermic and low temperature is conducive to the adsorption process. Positive  $\Delta S$  values were calculated, demonstrating an increase in the adsorption disorder of TMP onto the adsorbent.

3.6. Orthogonal experiment

The orthogonal experiment design and analysis method is the most commonly used method for experimental optimization. An orthogonal experiment can be designed based on the actual level and number of factors that affect experimental results. In this study, a four factor and three level orthogonal experiments was employed to find the dominant factor that affects the removal rate and equilibrium adsorption capacity of TMP by AWAC. The four factors involved were dosage of AWAC, initial concentration of TMP solution, pH and temperature.

The orthogonal experiment design is shown in Table 6, including four factors at three levels, and the results are presented in Table 7. The order of the four factors influencing removal efficiency of TMP is pH > AWAC dosage > temperature > TMP solution concentration. For the adsorption capacity, the order is pH > TMP solution concentration > AWAC dosage > temperature. The optimal combination was determined as pH = 6, initial TMP concentration = 60 mg/L, temperature = 303 K and AWAC content = 1.0 g/L. The influence of pH on the adsorption capacity was higher than the other three factors.

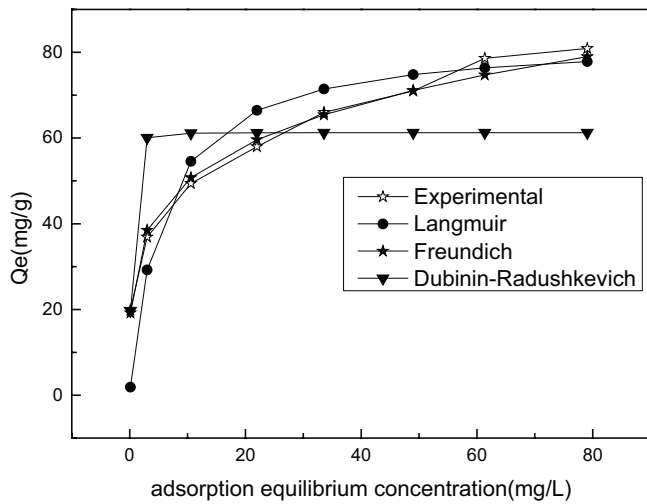


Fig. 9. Comparison of experimental data with models at 303 K.

Table 4  
Comparison of maximum adsorption capacities of various AC adsorbents for TMP

Absorbents	Maximum adsorption capacity (mg/g)	References
Spent brewery grains	30.50	[6]
Tea waste	85.16	[34]
Montmorillonite K10	89.90	[35]
AWAC	125.0	This work

3.7. Infrared spectra analysis

The functional groups on the surface of AWAC were determined by FTIR spectroscopy, and several different functional groups are present (Fig. 10). The adsorption peak at 400–1,000  $\text{cm}^{-1}$  was attributed to metal–oxygen and metal–hydroxyl vibrations [14]. The adsorption peak at 900–1,300  $\text{cm}^{-1}$  was ascribed to phosphorus-containing functional groups, which originated from the phosphoric acid activation employed during the preparation process [13]. The peak at 1,571  $\text{cm}^{-1}$  indicated asymmetric stretching vibration of  $-\text{COO}^-$  groups. The peaks in the 1,000–1,200  $\text{cm}^{-1}$  range were assigned to the C–C vibrations of esters. The functional group vibrations responsible for the 1,042  $\text{cm}^{-1}$  peak were primer alcohol stretching vibrations. The peak around 400–600  $\text{cm}^{-1}$  revealed the presence of C–H groups. Peak intensities from the surface of the activated carbon decreased after adsorption, and it may be that the functional groups on the surface of the activated carbon reacted with TMP or were obscured by adsorbed TMP.

Table 5  
Thermodynamic parameters for the adsorption of TMP onto alligator weed-activated carbon

Temperature (K)	K (L/mol)	$\Delta G^\circ$ (kJ/mol)	$\Delta S^\circ$ (J/mol K)	$\Delta H^\circ$ (kJ/mol)
298	20,901	-12.85		
303	51,940	-13.07	86	-1.124
308	51,176	-13.25		

Table 6  
Results of orthogonal experimental design

	pH	Temperature (T)	Concentration (mg/L)	Dosage (g/L)	Removal rate (%)	Equilibrium amount (mg/g)
1	2	298	60	0.03	40.2	39.6
2	2	303	80	0.04	47.7	49.2
3	2	308	100	0.05	45.5	45.9
4	4	298	80	0.05	68.7	55.3
5	4	303	100	0.03	43.9	76.1
6	4	308	60	0.04	39.7	49.6
7	6	298	100	0.04	78.4	95.3
8	6	303	60	0.05	95.0	55.5
9	6	308	80	0.03	73.5	58.3

Table 7  
Results of orthogonal experiments

	Level	pH	Temperature (K)	Concentration (mg/L)	Dosage (g/L)
Adsorption rate	K1	133.4	187.3	174.9	157.6
	K2	129.1	186.6	189.9	165.8
	K3	246.9	158.7	167.8	209.2
	$\bar{K1}$	44.47	62.43	58.30	52.53
	$\bar{K2}$	43.03	62.20	63.30	55.27
	$\bar{K3}$	82.30	52.90	55.93	69.73
	R	39.27	9.53	7.37	17.2
Adsorption quantity	K1	134.7	190.2	144.7	174.0
	K2	181.0	180.8	162.8	194.1
	K3	209.1	153.8	217.3	156.7
	$\bar{K1}$	44.90	63.40	48.23	58.00
	$\bar{K2}$	60.33	60.27	54.27	64.70
	$\bar{K3}$	69.70	51.27	72.43	52.23
	R	24.80	12.13	24.20	12.47

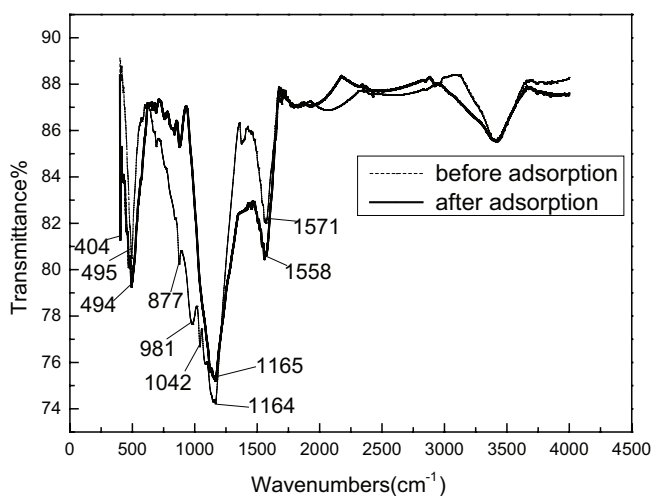


Fig. 10. Fourier transforms infrared spectra of the AWAC before and after TMP adsorption.

#### 4. Conclusions

AWAC prepared using phosphoric acid activation could adsorb TMP from solution efficiently. SEM analysis showed that the surface of the AWAC had developed micropores and mesopores. The BET surface area of AWAC was determined as 752.6 m<sup>2</sup>/g, and the average pore size was 5.80 nm, which were responsible for its favorable adsorption ability. The experimental kinetic data of TMP sorption by AWAC fitted better to the pseudo-second-order kinetic equation, indicating the rate-limiting factor was bond formation between the TMP and AWAC. The maximum adsorption capacity of TMP by AWAC was ~125 mg/g at 298 K. The experimental adsorption isothermal data conformed preferably to the Freundlich model, with a  $R^2$  of 0.9950, which indicates multimolecular layer adsorption. Thermodynamic studies revealed that the adsorption process is spontaneous and exothermic. FTIR spectroscopy identified the AWAC surface functional groups, such as C–H, C–O and C–C moieties. The intensity of the FTIR spectral peaks of AWAC decreased after adsorption, owing to reaction of the functional groups with TMP. Our results could provide insightful information to design and optimize effluent treatment facilities, and adsorption of TMP on low-cost activated carbon prepared from alligator weed has a promising application.

#### Acknowledgments

This work was supported by the Promotional research fund for excellent young and middle-aged scientists of Shandong Province (No. BS2014HZ019), the China Postdoctoral Science Foundation (No. 2014M551950), a Project of Shandong Province Higher Educational Science and Technology Program (No. J15LE07 and No. J15LH06), Natural Science Foundation of Shandong Province (No. ZR2016DM09) and the Major Science and Technology Program for Water Pollution Control and Treatment (No. 2012ZX07203004, 2015ZX07203005 and 2015ZX07203-007-005).

#### References

- [1] S.H. Kim, H.K. Shon, H.H. Ngo, Adsorption characteristics of antibiotics trimethoprim on powdered and granular activated carbon, *J. Ind. Eng. Chem.*, 16 (2010) 344–349.
- [2] P.F. Pereira, W.P. da Silva, R.A.A. Muñoz, E.M. Richter, A simple and fast batch injection analysis method for simultaneous determination of phenazopyridine, sulfamethoxazole,

- and trimethoprim on boron-doped diamond electrode, *J. Electroanal. Chem.*, 766 (2016) 87–93.
- [3] R. Hirsch, T. Ternes, K. Haberer, K.L. Kratz, Occurrence of antibiotics in the aquatic environment, *Sci. Total Environ.*, 225 (1999) 109–118.
- [4] H. Liu, J. Zhang, N. Bao, C. Cheng, L. Ren, C. Zhang, Textural properties and surface chemistry of lotus stalk-derived activated carbons prepared using different phosphorus oxyacids: adsorption of trimethoprim, *J. Hazard. Mater.*, 235–236 (2012) 367–375.
- [5] H. Liu, J. Zhang, L. Jiang, Y. Kang, C. Cheng, Z. Guo, C. Zhang, Development of carbon adsorbents with high surface acidic and basic group contents from phosphoric acid activation of xylitol, *RSC Adv.*, 5 (2015) 81220–81228.
- [6] Z. Bekçi, Y. Seki, M. Kadir Yurdakoç, A study of equilibrium and FTIR, SEM/EDS analysis of trimethoprim adsorption onto K10, *J. Mol. Struct.*, 827 (2007) 67–74.
- [7] X. Bai, K. Acharya, Removal of trimethoprim, sulfamethoxazole, and triclosan by the green alga *Nannochloris* sp., *J. Hazard. Mater.*, 315 (2016) 70–75.
- [8] P.K. Gautam, R.K. Gautam, S. Banerjee, G. Lofrano, M.A. Sanroman, M.C. Chattopadhyaya, J.D. Pandey, Preparation of activated carbon from Alligator weed (*Alternanthera philoxeroides*) and its application for tartrazine removal: isotherm, kinetics and spectroscopic analysis, *J. Environ. Chem. Eng.*, 3 (2015) 2560–2568.
- [9] X.S. Wang, Y.P. Tang, S.R. Tao, Kinetics, equilibrium and thermodynamic study on removal of Cr (VI) from aqueous solutions using low-cost adsorbent Alligator weed, *Chem. Eng. J.*, 148 (2009) 217–225.
- [10] S. Schooler, Z. Baron, M. Julien, Effect of simulated and actual herbivory on alligator weed, *Alternanthera philoxeroides*, growth and reproduction, *Biol. Control*, 36 (2006) 74–79.
- [11] X.S. Wang, B. Zhang, Sorption of Al (III) from aqueous solution by fresh macrophyte alligator weed: equilibrium and kinetics, *Desalination*, 250 (2010) 485–489.
- [12] I.E. Bassett, Q. Paynter, J.R. Beggs, Invertebrate community composition differs between invasive herb alligator weed and native sedges, *Acta Oecol.*, 41 (2012) 65–73.
- [13] M.-S. Miao, Q. Liu, L. Shu, Z. Wang, Y.-Z. Liu, Q. Kong, Removal of cephalixin from effluent by activated carbon prepared from alligator weed: kinetics, isotherms, and thermodynamic analyses, *Process Saf. Environ. Prot.*, 104 (2016) 481–489.
- [14] Q. Kong, Y.-n. Wang, L. Shu, M.-s. Miao, Isotherm, kinetic, and thermodynamic equations for cephalixin removal from liquids using activated carbon synthesized from loofah sponge, *Desal. Wat. Treat.*, 57 (2015) 7933–7942.
- [15] J. Fan, J. Zhang, C. Zhang, L. Ren, Q. Shi, Adsorption of 2,4,6-trichlorophenol from aqueous solution onto activated carbon derived from looestrife, *Desalination*, 267 (2011) 139–146.
- [16] E.K. Putra, R. Pranowo, J. Sunarso, N. Indraswati, S. Ismadi, Performance of activated carbon and bentonite for adsorption of amoxicillin from wastewater: mechanisms, isotherms and kinetics, *Water Res.*, 43 (2009) 2419–2430.
- [17] L. Lü, D. Lu, L. Chen, F. Luo, Removal of Cd(II) by modified lawn grass cellulose adsorbent, *Desalination*, 259 (2010) 120–130.
- [18] S.M. Yakout, G. Sharaf El-Deen, Characterization of activated carbon prepared by phosphoric acid activation of olive stones, *Arabian J. Chem.*, 9 (2016) S1155–S1162.
- [19] H. Liu, J. Zhang, C. Zhang, N. Bao, C. Cheng, Activated carbons with well-developed microporosity and high surface acidity prepared from lotus stalks by organophosphorus compounds activations, *Carbon*, 60 (2013) 289–291.
- [20] M.M. Hamed, M.M. Ali, M. Holiel, Preparation of activated carbon from doum stone and its application on adsorption of  $^{60}\text{Co}$  and  $^{152+154}\text{Eu}$ : equilibrium, kinetic and thermodynamic studies, *J. Environ. Radioact.*, 164 (2016) 113–124.
- [21] Y. Sun, H. Li, G. Li, B. Gao, Q. Yue, X. Li, Characterization and ciprofloxacin adsorption properties of activated carbons prepared from biomass wastes by  $\text{H}_3\text{PO}_4$  activation, *Bioresour. Technol.*, 217 (2016) 239–244.
- [22] H. Liu, X. Wang, G. Zhai, J. Zhang, C. Zhang, N. Bao, C. Cheng, Preparation of activated carbon from lotus stalks with the mixture of phosphoric acid and pentaerythritol impregnation and its application for Ni(II) sorption, *Chem. Eng. J.*, 209 (2012) 155–162.
- [23] L. Wang, J. Zhang, R. Zhao, C. Zhang, C. Li, Y. Li, Adsorption of 2,4-dichlorophenol on Mn-modified activated carbon prepared from *Polygonum orientale* Linn, *Desalination*, 266 (2011) 175–181.
- [24] U. Kuila, M. Prasad, Specific surface area and pore-size distribution in clays and shales, *Geophys. Prospect.*, 61 (2013) 341–362.
- [25] C. Wu, J. Gao, Q. Zhao, Y. Zhang, Y. Bai, X. Wang, X. Wang, Preparation and supercapacitive behaviors of the ordered mesoporous/microporous chromium carbide-derived carbons, *J. Power Sources*, 269 (2014) 818–824.
- [26] Z. Qi, Q. Liu, Z.R. Zhu, Q. Kong, Q.F. Chen, C.S. Zhao, Y.Z. Liu, M.S. Miao, C. Wang, Rhodamine B removal from aqueous solutions using loofah sponge and activated carbon prepared from loofah sponge, *Desal. Wat. Treat.*, 57 (2016) 29421–29433.
- [27] L.F. Delgado, P. Charles, K. Glucina, C. Morlay, Adsorption of ibuprofen and atenolol at trace concentration on activated carbon, *Sep. Sci. Technol.*, 104 (2014) 420–424.
- [28] R. Nadeem, M.N. Zafar, A. Afzal, M.A. Hanif, R. Saeed, Potential of NaOH pretreated *Mangifera indica* waste biomass for the mitigation of Ni(II) and Co(II) from aqueous solutions, *J. Taiwan Inst. Chem. Eng.*, 45 (2014) 967–972.
- [29] K. Chandra Sekhar, C.T. Kamala, N.S. Chary, Y. Anjaneyulu, Removal of heavy metals using a plant biomass with reference to environmental control, *Int. J. Miner. Process.*, 68 (2003) 37–45.
- [30] H. Liu, J. Zhang, N. Bao, C. Cheng, L. Ren, C. Zhang, Textural properties and surface chemistry of lotus stalk-derived activated carbons prepared using different phosphorus oxyacids: adsorption of trimethoprim, *J. Hazard. Mater.*, 235–236 (2012) 367–375.
- [31] V.N. Singh, G. Prasad, K.K. Panday, Use of wollastonite for the treatment of Cu(II) rich effluents, *Water Air Soil Pollut.*, 27 (1986) 287–296.
- [32] N.A. Oladoja, C.O. Aboluwoye, Y.B. Oladimeji, Kinetics and isotherm studies on Methylene Blue adsorption onto ground palm kernel coat, *Turk. J. Eng. Environ. Sci.*, 32 (2008) 303–312.
- [33] F.O. Okeola, E.O. Odeunmi, Freundlich and Langmuir isotherms parameters for adsorption of methylene blue by activated carbon derived from agrowastes, *Adv. Nat. App. Sci.*, 4 (2010) 281–288.
- [34] J. Pedro Silva, S. Sousa, J. Rodrigues, H. Antunes, J.J. Porter, I. Gonçalves, S. Ferreira-Dias, Adsorption of acid orange 7 dye in aqueous solutions by spent brewery grains, *Sep. Purif. Technol.*, 40 (2004) 309–315.
- [35] M.T. Uddin, M.A. Islam, S. Mahmud, M. Rukanuzzaman, Adsorptive removal of methylene blue by tea waste, *J. Hazard. Mater.*, 164 (2009) 53–60.
- [36] F. Nekouei, H. Kargarzadeh, S. Nekouei, I. Tyagi, S. Agarwal, V. Kumar Gupta, Preparation of Nickel hydroxide nanoplates modified activated carbon for Malachite Green removal from solutions: kinetic, thermodynamic, isotherm and antibacterial studies, *Process Saf. Environ. Prot.*, 102 (2016) 85–97.
- [37] I.A. Rahman, B. Saad, S. Shaidan, E.S.S. Rizal, Adsorption characteristics of malachite green on activated carbon derived from rice husks produced by chemical-thermal process, *Bioresour. Technol.*, 96 (2005) 1578–1583.